

On modelling of density driven flow

P. ACKERER, A. YOUNES

Institute of Fluid Mechanics, 2 Rue Boussingault, F-67000 Strasbourg, France
e-mail: ackerer@imf.u-strasbg.fr

S. E. OSWALD & W. KINZELBACH

Institute of Hydromechanics and Water Resources Management, Swiss Federal Institute, HIL G 37.3, CH-8093 Zürich-Hoenggerberg, Switzerland.

Abstract Numerous questions are still open in the modelling of density driven flow. These questions address the mathematical formulation of the mass balance equations and the numerical resolution of these nonlinear coupled equations. An attempt at model validation is made by simulating two test cases with a new numerical code based on mixed and discontinuous finite elements. First, the Elder test case is simulated with different formulation of the mass balance equations. Second, a simulation of a three-dimensional (3-D) laboratory experiment is run without any calibration. For both computations, very similar results are obtained using the complete fluid mass balance equation and the fluid mass balance equation obtained by neglecting the density gradient in space. Both models fail in the simulation of the 3-D experiment.

INTRODUCTION

A large amount of theoretical work has been done to improve mathematical models. At the same time, a lot of numerical models have been developed. However, the need for accurate models to simulate the transport of salt water continues to increase due to a large number of environmental problems such as saltwater intrusion in exploited coastal aquifers or aquifers overlying salt formations, leakage from landfills, and disposal of radioactive or toxic wastes in salt rock formations. Numerous two-dimensional (2-D) benchmarks (the Henry, Elder and Salt Dome test cases) have been used to compare the accuracy of mathematical models and numerical codes. Their validity is still under debate and the need for well-defined experiments is very high.

The most common mathematical models and some standard assumptions are presented. Simulations of the Elder problem help in the selection of the mathematical models. These models are used to simulate a detailed three-dimensional (3-D) laboratory experiment.

MATHEMATICAL MODELS AND STANDARD ASSUMPTIONS

The more common mathematical models of brine transport in porous media are based on the work of Bear (1972). The proposed model has been widely discussed by Lever & Jackson (1985), Hassanizadeh & Leijnse (1988), and Kolditz *et al.* (1997), among others. The expressions for the balance equations are:

- Mass balance of the fluid:

$$\frac{\partial(\varepsilon\rho)}{\partial t} + \nabla \cdot (\varepsilon\rho\mathbf{v}) = \rho Q \quad (1)$$

- Momentum balance (generalized Darcy's law):

$$\mathbf{v} = -\frac{\mathbf{k}}{\varepsilon\mu} \cdot (\nabla P + \rho\mathbf{g}\nabla z) \quad (2)$$

- Solute mass conservation (in terms of mass fraction):

$$\frac{\partial(\varepsilon\rho\omega)}{\partial t} + \nabla \cdot (\varepsilon\rho\omega\mathbf{v}) - \nabla \cdot (\varepsilon\rho\mathbf{D}\cdot\nabla\omega) = Q_\omega \quad (3)$$

where the dispersive tensor is given by:

$$\mathbf{D} = D_m \mathbf{I} + (\alpha_L - \alpha_T) \mathbf{v}\mathbf{v}/|\mathbf{v}| + \alpha_T |\mathbf{v}|\mathbf{I} \quad (4)$$

where: P fluid pressure [$\text{M L}^{-1} \text{T}^{-2}$], \mathbf{v} fluid velocity [L T^{-1}], ε porosity [-], \mathbf{k} permeability tensor [L^2], \mathbf{g} gravity acceleration [L T^{-2}], ρ fluid density [M L^{-3}], μ fluid dynamic viscosity [$\text{M L}^{-1} \text{T}^{-1}$], ω solute mass fraction [-], α_L , α_T longitudinal and transverse coefficient of mechanical dispersion [L], D_m pore water diffusion coefficient [$\text{L}^2 \text{T}^{-1}$], \mathbf{I} unit tensor. The associated boundary conditions of equations (1) and (3) are of Dirichlet, Neuman or mixed type. These equations are coupled by the following linearized state equation, assuming that the viscosity remains constant:

$$\rho = \rho_0 \left(1 + \frac{\rho_s - \rho_0}{\rho_0} \omega \right) \quad (5)$$

where ρ_s is the fluid density at saturation and ρ_0 the density of pure water. Combining equations (1) and (2) and assuming that the effect of temperature can be neglected, the solid matrix is rigid and immobile and that the porosity is only a function of pressure, leads to the standard flow equation:

$$\rho S_p \frac{\partial P}{\partial t} + \varepsilon \frac{\partial \rho}{\partial \omega} \frac{\partial \omega}{\partial t} - \nabla \cdot \left[\rho \frac{\mathbf{k}}{\mu} \cdot (\nabla P + \rho\mathbf{g}\nabla z) \right] = \rho Q \quad (6)$$

Following Huyakorn *et al.* (1987), this can also be written in terms of head by:

$$S \frac{\partial h}{\partial t} + \varepsilon \frac{(\rho_s - \rho_0)}{\rho_0} \frac{\partial \omega}{\partial t} - \nabla \cdot \left[\mathbf{K} (\nabla h + \frac{(\rho - \rho_0)}{\rho_0} \nabla z) \right] = \frac{\rho}{\rho_0} Q \quad (7)$$

where $h = P/\rho_0 g + z$, $\mathbf{K} = \mathbf{k}\rho g/\mu$, \mathbf{K} is the hydraulic conductivity tensor [L T^{-1}] and $S = \rho g S_p$, the specific storage [L^{-1}].

In order to reduce the degree of coupling between the three first equations, and therefore reduce drastically the computer time, two standard assumptions have been proposed:

- the Oberbeck-Boussinesq (Oberbeck, 1879; Boussinesq, 1903) (OB) approximation where density variations are neglected in the fluid mass balance:

$$\frac{\partial \varepsilon}{\partial t} + \nabla \cdot (\varepsilon\mathbf{v}) = Q \quad (8)$$

- the density variation in the fluid flow direction is neglected (Bear, 1972), and the fluid mass conservation can be written:

$$\frac{\partial(\varepsilon\rho)}{\partial t} + \rho\nabla\cdot(\varepsilon\mathbf{v}) = \rho Q \quad (9)$$

NUMERICAL TECHNIQUES

Numerous codes have already been developed based on various finite volume approaches (finite differences, finite elements) or combination of two distinct techniques like method of characteristics and finite differences (e.g. Konikow *et al.*, 1997). As stated by Diersch & Kolditz (1998), the success of a numerical solution for variable density flow problems is essentially dependent on evaluating Darcy fluxes for a given discretization. To improve the accuracy of the velocity computation, we use the mixed hybrid finite elements approximation (Chavent & Roberts, 1991) which is a good method for solving the groundwater flow problem. Indeed, this approximation gives a velocity throughout the field and the normal component of the velocity is continuous across the inter-element boundaries. Moreover, the interpolation function of the velocities is given *a priori* in the numerical development and no additional assumptions are required.

For the solute transport equation, we use a combination of discontinuous and mixed hybrid finite elements. Upwind discontinuous finite elements coupled with a slope limiting technique (Toro, 1997) are well suited to solve the hyperbolic part of the transport equation. Mixed hybrid finite element ensures an accurate computation of dispersive fluxes (Siegel *et al.*, 1997). Dirichlet boundary conditions can be reproduced in a finite differences (average value over an element) or finite element (prescribed value at the node) way (Younès *et al.*, 1999).

A detailed presentation in 2-D of both methods applied to density driven flow simulations can be found in Ackerer *et al.* (1999). An explicit scheme is used for the convective part of the solute transport equation, an implicit scheme for its dispersive part. Due to the explicit scheme, the Courant criterion has to be fulfilled which can lead to very small time steps. In order to reduce the CPU time, the computation of advection and dispersion is performed only for the elements where the mass exchange exceeds a prescribed value, i.e. in the mixing zones. This can lead to a drastic reduction in CPU time, especially for irregular meshes.

In this simulator, named TVDV-3D for Transport with Variable Density and Viscosity, the flow and transport equations are solved in a sequential way using a standard fixpoint (Picard) scheme. The density of the new iteration is calculated from the mass fraction of the previous iteration step. The stopping criterion is based on the maximum value of the residual. The differences between this stopping criterion and a criterion based on the maximum change in the primary variables are discussed in Ackerer *et al.* (1999).

These techniques have been used to simulate the Elder problem with the following fluid balance equations: equation (1) referred to as case 1, equation (9) referred to as case 2, and equation (8) referred to as case 3 (OB model).

THE ELDER PROBLEM

The Elder problem (Elder, 1966) is a free convection problem where fluid flow is driven purely by fluid density differences. It involves total density variations of 20%, which makes this a strongly coupled flow case. This test case has been widely studied (Voss & Souza, 1987; Oldenburg & Pruess, 1995; Kolditz et al., 1997; Ackerer et al., 1999; among others). The parameters for the problem are given in Table 1.

Table 1 Parameters for the Elder problem.

Permeability	$k_x = k_y = 4.845 \cdot 10^{-13} \text{ (m}^2\text{)}$
Porosity	$\epsilon = 0.1 \text{ (-)}$
Dispersivity	$\alpha_L = \alpha_T = 0 \text{ (m)}$
Molecular diffusion coefficient	$D_m = 3.565 \cdot 10^{-6} \text{ (m}^2 \text{ s}^{-1}\text{)}$
Dynamic viscosity	$\mu = 10^{-3} \text{ (Pa s}^{-1}\text{)}$
State equation	$\rho = \rho_0 + 200\omega$

The domain and boundary conditions are shown in Fig. 1. The results obtained by the three models are presented in Fig. 2. As stated by Kolditz et al. (1997), the OB model (case 3) is not valid. However, it is interesting to notice that, although the concentration distribution is different for 10 years for the OB model, it is very similar for 20 years. No significant differences can be found between the simulation performed with equation (1) and equation (9). The computations were run on a PW600 Digital Workstation with an alpha processor of 600 MHz. The fully coupled model (case 1) required more CPU time (720 s) because of its higher nonlinear behaviour and because the resolution of equation (1) leads to an asymmetrical matrix. The numerical resolution of equations (8) and (9) leads to a symmetrical matrix. The differences in CPU time between case 2 (464 s) and case 3 (393 s) are due to a higher coupling for case 2.

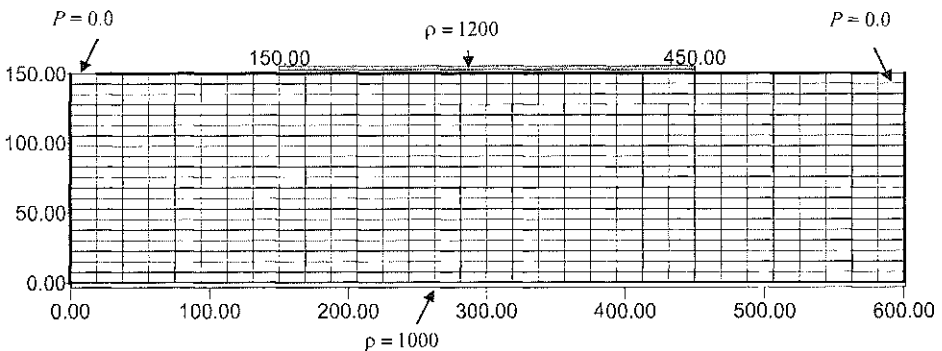


Fig. 1 Domain and boundary conditions for the Elder problem.

THE SALTPPOOL PROBLEM

A 3-D experiment, called the Saltpool experiment, conducted by Oswald (1998) will be used to verify the 3-D numerical code. The experiments have been done on a cube of

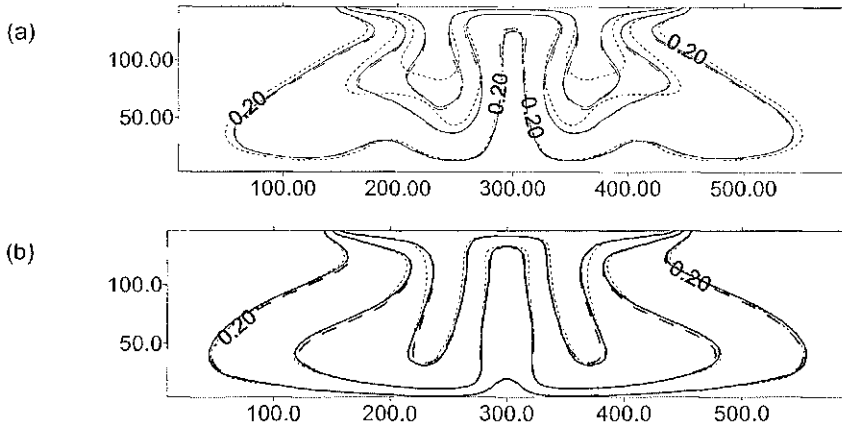


Fig. 2 Simulated concentration at (a) $t = 10$ years and (b) $t = 20$ years. — Case 1 (720 s), --- Case 2 (464 s), ... Case 3 (393 s).

dimensions $0.20 \times 0.20 \times 0.20 \text{ m}^3$. The cube is filled with glass beads and saturated with pure water. The five openings are squares of dimension $0.001 \times 0.001 \text{ m}^2$ (Fig. 3). The experiments are run in 3 steps:

- step 1: injection of the salt water by the opening 5. The outflow is at openings 1 to 4.
- step 2: no injection. All openings are closed.
- step 3: injection at opening 4. Outflow at opening 2, the others are closed.

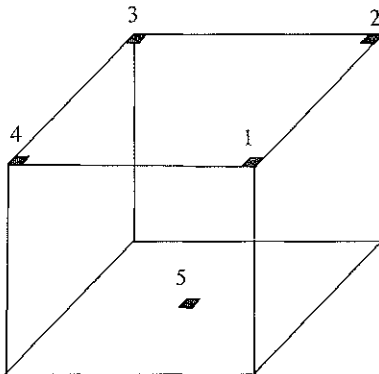


Fig. 3 The experimental cube and its openings.

Two experiments will be simulated with the experimental conditions given in Oswald (1998), Saltp-L with an input mass fraction of 1.0% and Saltp-D with an input mass fraction of 10%.

For steps 1 and 3, the flow rate is prescribed at the injection, a pressure equal to zero is prescribed at the outflow. Prescribed pressure, injection flux and concentration are given at element faces which have an area of $0.0015 \times 0.0015 \text{ m}^2$ which is greater than the size of the openings. This approximation is analysed at the end of the paper. Oswald (1998) measured the flow and transport parameters by additional experiments done on columns or on the same cube with the same filling. These parameters are used for the simulations (Table 2).

Table 2 Flow and transport parameters used for the simulations.

Permeability	$9.8 \times 10^{-10} \text{ (m}^2\text{)}$
Porosity	0.37 (-)
Long. dispersivity	$1.2 \times 10^{-3} \text{ (m)}$
Trans. dispersivity/long. dispersivity	0.1 (-)
Molecular diffusion	$8.7 \times 10^{-10} \text{ (m}^2 \text{ s}^{-1}\text{)}$

The discretization of the cube is as follows: 15 elements in X and Y from length 0.0015 m (at the boundary) to 0.0195 m close to the centre, with an element size of 0.004 m in the middle to describe opening 5 and 12 elements in Z , with an element size from 0.007 m close to the top and bottom boundary to 0.02 m in the middle of the box. This leads to 2700 elements. Although the number of unknowns is more important for the resolution of advection ($8 \times$ number of elements), the CPU time required to compute the advective transport is negligible compared to the CPU time required for the resolution of the flow and/or dispersion equations for coupled problems. The relevant number of unknowns is therefore the number of element faces, which is equal to 8685.

Several different experiments have been performed under similar conditions. The same input mass fraction (10%) has been prescribed for experiments Saltp-D and SaltB-D. Two different fluid mass balance models are used to simulate the experiments performed with the highest concentration: equation (1) for Sim-1 and equation (9) for Sim-2. Experimental and simulated results are presented in Fig. 4.

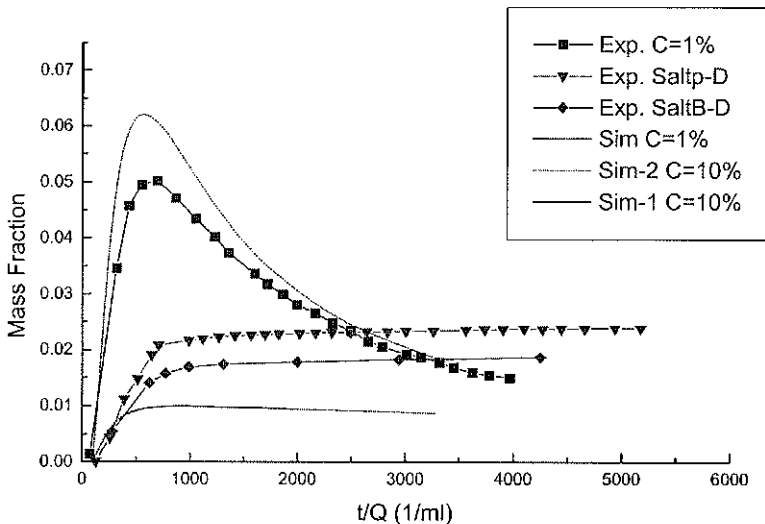


Fig. 4 Computed breakthrough curves at the outflow compared with the data measured by Oswald (1998).

Quite different results are obtained for the simulation of the experiments Saltp-L ($C = 1\%$) and Saltp-D ($C = 10\%$). The tendencies are quite similar: the beginning of the breakthrough curves are well reproduced but the maximum value is overestimated

for Saltp-L and underestimated for Saltp-D by the simulations. Both mathematical models provide very similar results.

Different computations have been run to improve the results:

- no significant change has been found by locally modifying the mesh size at the opening (from $0.0015 \times 0.0015 \text{ m}^2$ to $0.001 \times 0.001 \text{ m}^2$);
- the grid has been refined, which leads to a small decrease in the maximum simulated mass fraction;
- the permeability has been calibrated in order to reproduce the Saltp-L experiment. The match is quite good when the permeability is increased by 40% (Fig. 5). This new permeability value leads to a significant decrease of the maximum mass fraction reached by the simulation of experiment Saltp-D.

Oswald (1998) performed simulations of these experiments with a variety of codes to show the applicability of the experiments as a benchmark for verification of density driven flow codes. All these simulations show an overestimation of the maximum mass fraction for experiments Saltp-L and Saltp-D. Our results shown in Fig. 4 have the same quality as the best of the simulations shown for the Saltp-L experiment. For the Saltp-D simulations, they differ significantly. The closest simulation of the codes studied by Oswald (1998) reached a maximum value of about 0.05, whereas the maximum measured mass fraction is about 0.025. Our simulation reached a value of about 0.01, whereas the minimum measured mass fraction is about 0.015.

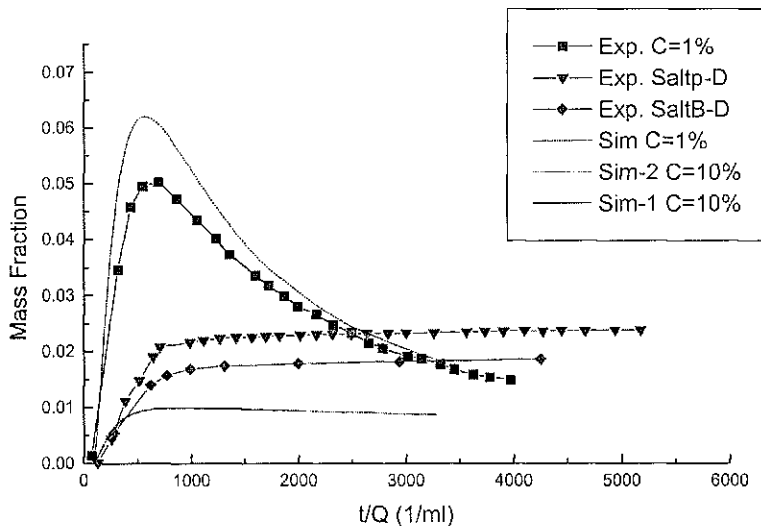


Fig. 5 Measured and computed breakthrough curves at the outflow. $K = 14 \cdot 10^{-10} \text{ m}^2$ for Sim C = 1% and C = 10%, $k = 9.810^{-10} \text{ m}^2$ for Sim-2).

CONCLUSIONS

The simulations done for the Elder and Saltpool test cases show that results obtained by neglecting the spatial density variations are very similar to those obtained with the complete fluid mass balance equation. The numerical resolution of the formulation

obtained by neglecting the spatial density variations leads to a symmetrical matrix whose resolution is faster than the resolution of the asymmetrical one obtained for the standard fluid mass balance equation.

The proposed 3-D model failed in the simulation of the Saltpool experiments. The extracted mass is overestimated by the simulation for the experiment performed with the low concentration, and underestimated for the experiment performed with the high concentration. We were able to improve the simulation of the low concentration experiment but the simulation of the high concentration became worse. These experiments are a real challenge for 3-D density driven flow models.

Acknowledgements This work was funded by the French National Research Centre (CNRS) and the INTAS Project no. 97-0068.

REFERENCES

- Ackerer, Ph., Younès, A. & Mosé, R. (1999) Modeling variable density flow and solute transport in porous medium: 1. Numerical model and verification. *Transport Porous Media* 35(3), 345–373.
- Bear, J. (1972) *Dynamics of Fluids in Porous Media*. Elsevier, New York.
- Boussinesq, J. (1903) Recherches théoriques sur l'écoulement des nappes d'eau infiltrées dans le sol et sur le débit des sources (Theoretical work on groundwater flow and flux at sources). *C.R.H. Acad. J. Math. Pures et Appliquées* 10, 5–78.
- Chavent, G. & Roberts, J. E. (1991) A unified physical presentation of mixed, mixed hybrid finite elements and standard finite difference approximations for the determination of velocities in water flow problems. *Adv. Wat. Resour.* 14(6), 329–348.
- Diersch, H. J. & Kolditz, O. (1998) Coupled groundwater flow and transport. 2. Thermoline and 3D convection systems. *Adv. Water Res.* 21, 401–425.
- Elder, J. W. (1966) Numerical experiments with a free convection in a vertical slot. *J. Fluid Mech.* 24, 823–843.
- Hassanizadeh, S. M. & Leijnse, A. (1988) On the modeling of brine transport in porous media. *Wat. Resour. Res.* 24(6), 321–330.
- Huyakorn, P. S., Andersen, P. F., Mercer, J. W. & White, J. R. (1987) Saltwater intrusion in aquifers: development and testing of a 3D finite element model. *Wat. Resour. Res.* 23(2), 293–312.
- Kolditz, O., Ratke, R., Diersch, H. J. & Zielke, W. (1997) Coupled groundwater flow and transport. 1. Verification of variable density flow and transport models. *Adv. Water Res.* 21(1), 27–46.
- Konikow, L. F., Sanford, W. E. & Campbell, P. J. (1997) Constant concentration boundary conditions: lessons from the HYDROCOIN variable-density groundwater benchmark problem. *Wat. Resour. Res.* 33(10), 2253–2261.
- Lever, D. A. & Jackson, C. P. (1985) On the equation for the flow of concentrated salt solution through a porous medium. *US Department of Energy, Report no. DOE/RW/85*.
- Oberbeck, A. (1879) Ueber die Wärmeleitung der Flüssigkeiten bei Berücksichtigung der Strömung infolge von Temperaturdifferenzen (On heat transport by fluids taking into account flow induced by temperature gradients). *Annalen der Physik und Chemie* 7, 271–292.
- Oldenburg, C. M. & Pruess, K. (1995) Dispersive transport dynamics in a strongly coupled groundwater-brine flow system. *Wat. Resour. Res.* 31(2), 289–302.
- Oswald, S. (1998) Dichteströmungen in porösen Medien: Dreidimensionale Experimente und Modellierung (Density driven flow in porous media: 3D experiments and modelling). PhD Thesis, ETH Zürich, Switzerland. Schriftenreihe IHW-002.
- Siegel, P., Mosé, R., Ackerer, Ph. & Jaffré, J. (1997) Solution of the advection dispersion equation using a combination of discontinuous and mixed finite elements. *Int. J. Numerical Methods in Fluids* 24, 595–613.
- Toro, E. F. (1997) *Riemann Solvers and Numerical Methods for Fluid Dynamics: A Practical Introduction*. Springer Verlag, Berlin, Germany.
- Voss, C. & Souza, W. R. (1987) Variable density flow and solute transport simulation of regional aquifers containing a narrow freshwater-saltwater transition zone. *Wat. Resour. Res.* 23(10), 1851–1866.
- Younès, A., Ackerer, Ph. & Mosé, R. (1999) Modeling variable density flow and solute transport in porous medium. 2. Re-evaluation of the salt dome flow problem. *Transport Porous Media* 35(3), 375–394.